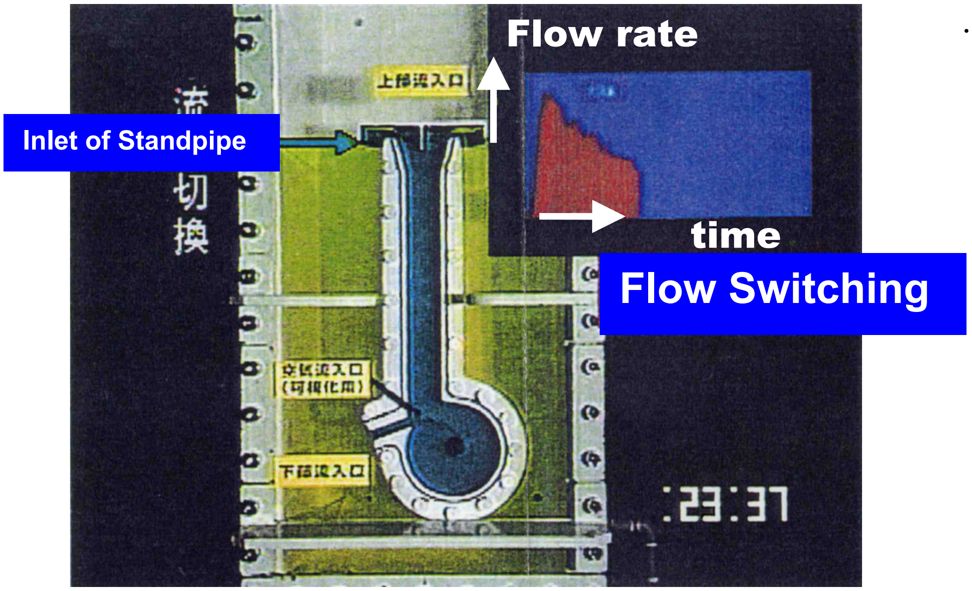

- 23.37 seconds after initiation of the test

Photo. 4.2.1-4 Flow Just before Large/Small Flow Switching

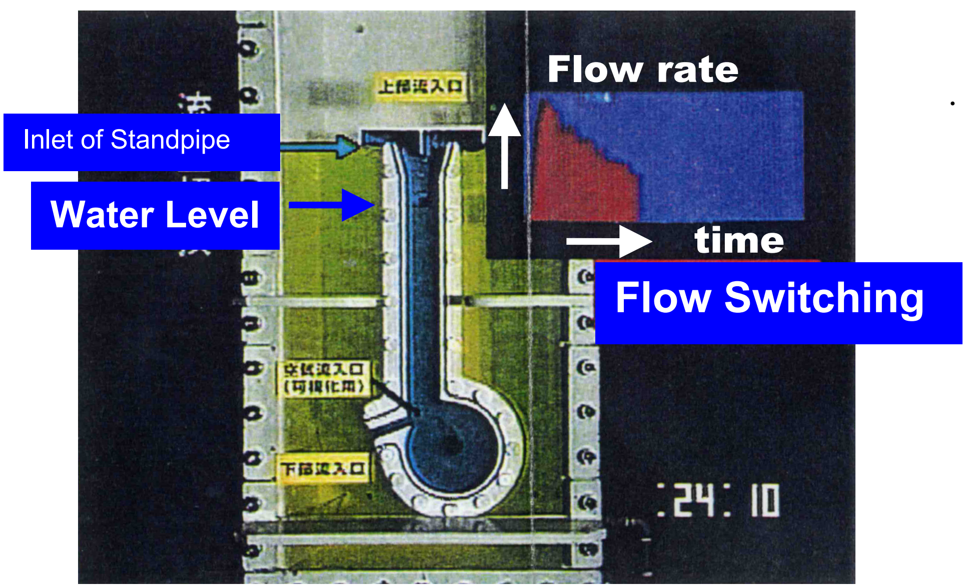

- 24.10 seconds after initiation of the test

Photo. 4.2.1-5 Flow Shortly after Large/Small Flow Switching

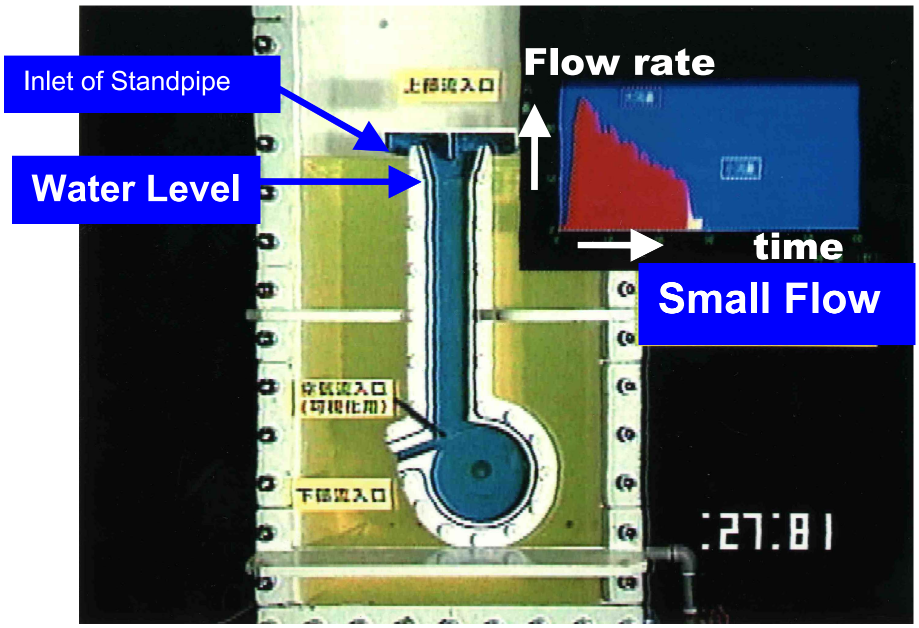

- 27.81 seconds after initiation of the test

Photo. 4.2.1-6 Flow during Small Flow

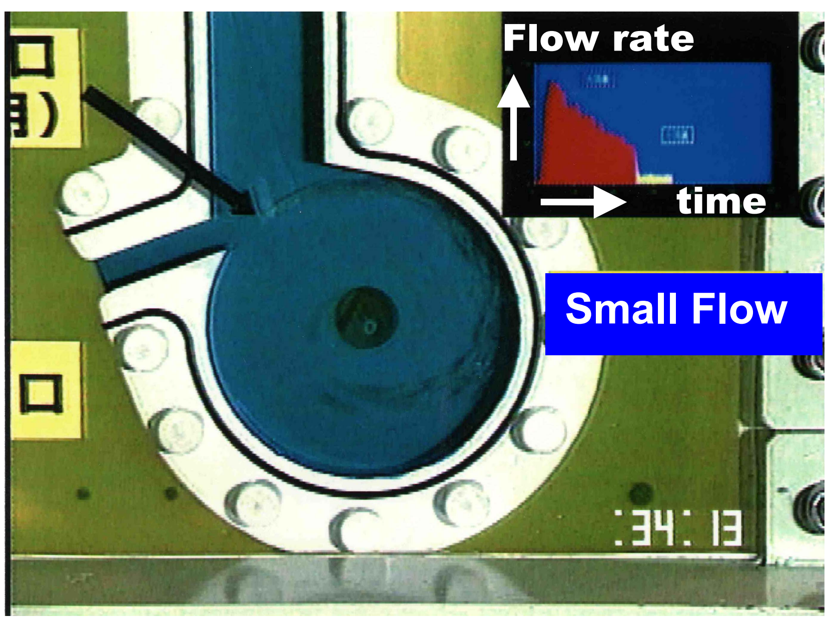

- 34.13 seconds after initiation of the test
- Air injection into the vortex chamber

(This Photo. shows that the vortex is formed in the vortex chamber.)

Photo. 4.2.1-7 Flow in the Vortex Chamber during Small Flow

4.2.2 1/3.5 Scale Test

1) Objectives

The ACC design uses an anti-vortex cap at the top of the standpipe to prevent the formation of a vortex as the flow drains from the tank such that the flow will only switch from a high flow to a lower flow when the level in the ACC tank drops below the top of the standpipe.

Without the anti-vortex cap, as the water level is reduced close to the upper end of the standpipe, it is possible for supercritical flow to form at the inlet of the standpipe and gas could be entrained, and the flow rate would not shift smoothly. The purpose of the experiments was to demonstrate that with the vortex cap design, a smooth flow switching behavior from the high flow to the lower flow as the tank level would decrease would occur.

The test was conducted to confirm the behavior of flow and potential for vortex formation in the ACC tank and confirming the effect of the anti-vortex cap.

2) Test apparatus

The outline drawing of the test facility is shown in Fig. 4.2.2-1. The test apparatus consists of the standpipe, test tank, pump and piping. The anti-vortex cap that is installed at the top of the standpipe was made of transparent acrylate such that the flow can be observed at the standpipe inlet. The scale of the standpipe inlet is 1/3.5 of the actual standpipe.

Fig. 4.2.2-1 Outline Drawing of 1/3.5 Scale Test Apparatus

3) Testing Method

(1) The experiment was scaled using the Froude Number as a basis since there was an open tank with a fluid surface. The relationship between the model tank (m) and the actual accumulator (p) is given below assuming the Froude Number is defined as

$$Fr = \frac{V}{(g \cdot L)^{0.5}} \qquad (4\text{-}2)$$

And $$Fr_p = Fr_m \qquad (4\text{-}3)$$

$$Q_p = \left(\frac{L_p}{L_m}\right)^{2.5} \cdot Q_m \qquad (4\text{-}4)$$

$$V_p = \left(\frac{L_p}{L_m}\right)^{0.5} \cdot V_m \qquad (4\text{-}5)$$

$$t_p = \left(\frac{L_p}{L_m}\right)^{0.5} \cdot t_m \qquad (4\text{-}6)$$

where

Fr	:	Froude number
L	:	Typical dimension
Q	:	Typical flow rate
V	:	Typical velocity
t	:	Time
p	:	Subscript of the actual ACC tank
m	:	Subscript of the 1/3.5 scale model

(2) The flow rate was measured by ultrasonic flow meter, and the tank water level was measured by the level marking on the sidewall of the tank.

4) Test condition

The test conditions are shown in Table 4.2.2-1. Two types of standpipe inlet (with the anti-vortex cap and without it) were tested. The tests were performed using two flow rates in which the test and actual ACC Froude numbers were preserved. The flow rates were [ ]and[ ] that covers the flow rates at flow switching at minimum initial gas pressure and at maximum initial gas pressure, respectively. The injection characteristics with test flow rates are shown in Fig. 4.2.2-2 to 4.2.2-5.

Table 4.2.2-1 Test Condition

Test Number	Test Condition			Remarks	Corresponding Actual Condition	
	Anti-vortex Cap	Flow Characteristics	Flow Rate just before switching (gpm (l/sec))		Initial Gas Pressure (psig (MPa(g)))	Flow Rate just before switching (gpm (m^3/h))
1-1	No	Fig. 4.2.2-2		Froude number is preserved.		
1-2	Yes	Fig. 4.2.2-3				
2-1	No	Fig. 4.2.2-4				
2-2	Yes	Fig. 4.2.2-5				

5) Parameters and measuring equipment

Flow rate and water level were measured to confirm the conditions during flow switching. The flow rate was measured by ultrasonic flow meter, and the tank water level was measured by the level marking on the sidewall of the tank.

6) Test results and consideration

Test results are listed in Table 4.2.2-2. The flow at the inlet for various conditions is shown in Photos. 4.2.2-1(1/2), (2/2) through 4.2.2-2(1/2), (2/2). The observations included.

(1) In the case of the standpipe inlet without the anti-vortex cap, when the water level is slightly decreased, a slight surface dimple appeared above the inlet and the initiation of supercritical flow developed. When the water level decreased further, the supercritical flow condition was apparent and the surface dimple reached into the standpipe, and gas entrainment occurred. (Photo. 4.2.2-1(1/2), (2/2))

(2) Below the water level where the supercritical flow condition becomes apparent, the critical depth became smaller consistent with the water level reduction. This resulted in lower flow rate and a slower reduction of the water level.

(3) The condition described in (2) above is apparent in the wave pattern. For example, in Fig. 4.2.2-2, supercritical flow was apparent and gas entrainment started at 26 seconds after initiation of the test, and the variation of the flow rate became bigger. As the flow rate became smaller, it took as long as 5 seconds until the flow rate into the standpipe became zero.

(4) This qualitative condition appeared in the case of both the minimum initial gas pressure of and the maximum initial gas pressure of without any significant differences.

(5) In the case of the standpipe inlet with the anti-vortex cap, a slight disturbance appeared on the water surface as the water level decreased from just above the upper end of the cap to the lower end of the cap. However, neither a vortex nor supercritical flow occurred, and the flow rate switched sharply in a short time. (Photos. 4.2.2-2(1/2), (2/2))
This condition is apparent in the wave pattern. For example, in Fig. 4.2.2-3, the flow rate into the standpipe became zero in approximately 1 second. The flow rate switched much

more quickly than the case without the anti-vortex cap (approximately 5 seconds, Fig.4.2.2-2).

(6) Based on the data and visual observation above, the desired effects of the anti-vortex cap were confirmed.

Table 4.2.2-2 List of Test Results

Test Number (T. No)	Test condition		Test Results		
	Flow Characteristics	Anti-vortex Cap	Vortex Formation	Finishing Transition time (sec)	Remark
1-1	Fig. 4.2.2-2	No	Yes	Approx. 5	Photo. 4.2.2-1(1/2), (2/2)
1-2	Fig. 4.2.2-3	Yes	No	Approx. 1	Photo. 4.2.2-2(1/2), (2/2)
2-1	Fig. 4.2.2-4	No	Yes	[ ]	-
2-2	Fig. 4.2.2-5	Yes	No	[ ]	-

Photo. 4.2.2-1 (1/2) Aspect of Flow without Anti-Vortex Cap (T. No. 1-1) 1/2

Photo. 4.2.2-1 (2/2) Aspect of Flow without Anti-Vortex Cap (T. No. 1-1) 2/2

Photo. 4.2.2-2 (1/2) Aspect of Flow with Anti-Vortex Cap (T. No. 1-2) 1/2

Photo 4.2.2-2(2/2) Aspect of Flow with Anti-Vortex Cap (T. No. 1-2) 2/2

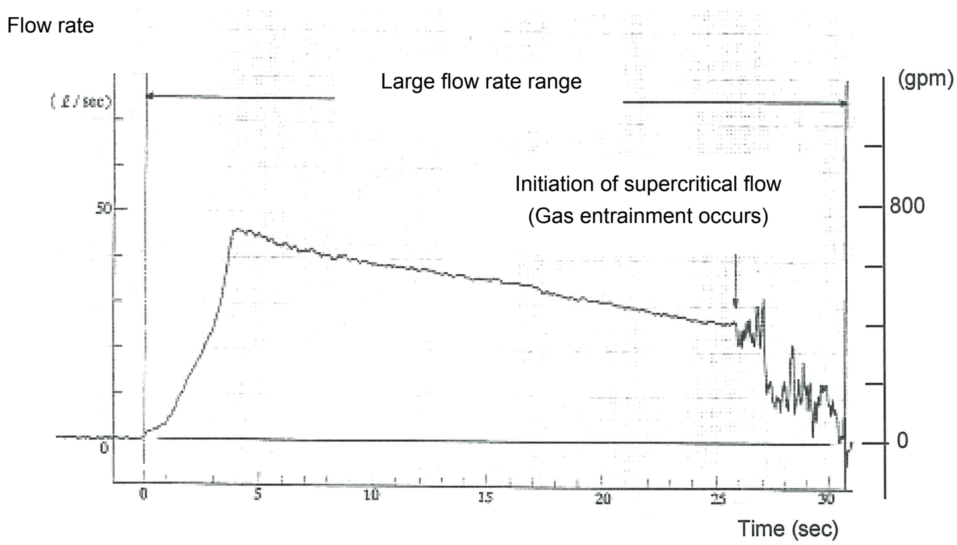

Fig 4.2.2-2 Test Flow Characteristics without Anti-Vortex Cap (T. No. 1-1)

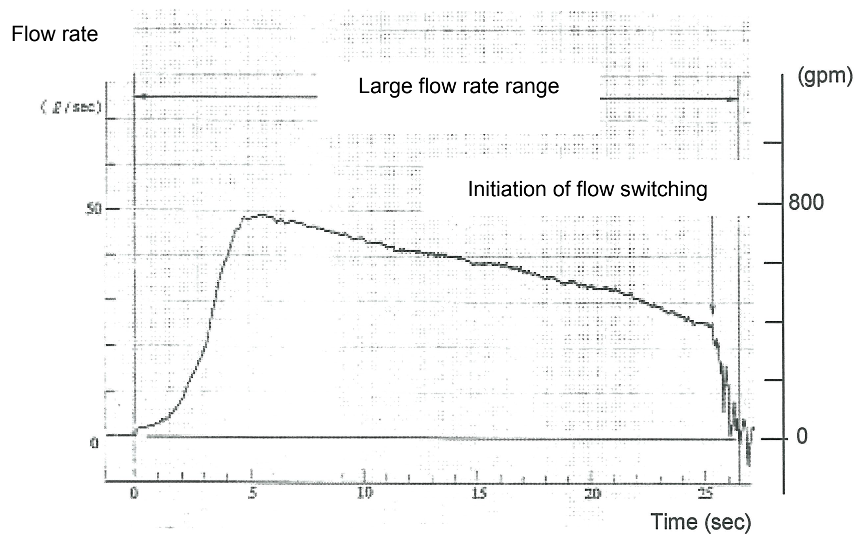

Fig 4.2.2-3 Test Flow Characteristics with Anti-Vortex Cap (T. No. 1-2)

Fig 4.2.2-4 Test Flow Characteristics without Anti-Vortex Cap (T. No. 2-1)

Fig 4.2.2-5 Test Flow Characteristics with Anti-Vortex Cap (T. No. 2-2)

4.2.3 1/5 Scale Test

1) Objectives

(1) Confirm the operational characteristics of the flow damper

Observation of the flow in the flow damper during large and small flow, large/small flow switching, and confirmation of the expected behavior of the flow

(2) Confirm the performance characteristics during large and small flow by measurement

The cavitation factor and flow rate coefficient during both flow conditions were measured, and confirm the flow characteristics are similar to the expected ACC performance. The flow characteristics obtained by the test were compared with the results of the full height 1/2 scale test later in this report and are used to confirm the validity of applying the scaling basis for these experiments.

2) Test apparatus

The outline drawings of the test apparatus is shown in Fig. 4.2.3-1. The test facility consists of a test tank, flow damper, standpipe, injection piping and exhaust tank. The flow damper made of transparent acrylate was installed outside of the test tank, thereby allowing fluid characteristics in the flow damper to be observed. A ball valve (nominal diameter is is provided on the injection line as the isolation valve and a gate valve (nominal diameter is is also provided on the injection line to control the flow resistance.

Fig. 4.2.3-1 Outline Drawing of the Visualization Test Apparatus

The specifications of the test facility are as follows:

(1) Test tank

Design Pressure :
Diameter :
Height :
Volume :

(2) Flow damper and standpipe (1/5 scale of the Actual size)

Diameter of vortex chamber :
Height of vortex chamber :
Shape of standpipe :

(3) Injection piping

Inner diameter :
(Simulating the pressure drop)

(4) Exhaust tank

Design Pressure :
Diameter :
Height :
Volume :

3) Testing method

(a) Visualization test method

(1) Visualization tests were conducted for three cases: (i) examining flow characteristics during large flow injection and flow switching, setting the initial pressure at [ ], which is the maximum design pressure of the test tank; (ii) examining flow characteristics during small flow injection, setting the initial pressure at [ ] for a long small flow injection time, and (iii) examining flow characteristics during flow switching, setting the initial pressure at [ ], which has the same Froude number as that of the actual plant condition.
(2) The flow characteristics in the flow damper were recorded and observed using a video camera, shown in Fig.4.2.3-1.
(3) The characteristics of the flow in the vortex chamber were observed using blue ink as a flow tracer.

(b) Low pressure injection testing method

(1) The test tank pressure, test tank water level, damper outlet pressure, and exhaust tank pressure were measured and input into a PC to calculate the flow rate coefficient and the cavitation factor.

(2) Flow rate coefficient and cavitation factor were obtained by the following equations:

Flow rate coefficient C_V

$$C_V = \frac{1}{\sqrt{K_D}} \tag{4-7}$$

$$K_D = \frac{(P_A + \rho g H) - (P_D + \rho {V_D}^2 / 2 + \rho g H')}{\rho V_D^2 / 2} \tag{4-8}$$

Cavitation factor σ_v

$$\sigma_v = \frac{P_D + P_{at} - P_v}{(P_A + \rho g H) - (P_D + \rho V_D^2 / 2 + \rho g H')} \tag{4-9}$$

Where

K_D	:	Resistance coefficient of flow damper
P_A	:	Test tank pressure [gage]
ρ	:	Density of water
g	:	Acceleration of gravity
H	:	Distance between test tank water level and vortex chamber
H'	:	Distance between outlet pipe and vortex chamber
P_{at}	:	Atmospheric pressure
P_v	:	Vapor pressure of water
P_D	:	Static pressure of flow damper outlet piping [gage] [Note]
V_D	:	Velocity in the flow damper outlet piping [Note]

Note: These parameters were the values converted to the scale of the actual ACC

(3) Data Processing

Data smoothing techniques were utilized to eliminate noises from data of the ACC water level, the ACC pressure and the flow damper outlet pressure data processing and is discussed.

The water level data as a function of time is shown here, and a polynomial equation is made by the least square method.

(a) Data of the ACC water level

The pressure data is shown as a function of time. a polynomial equation is made by the least square method.

(b) Data of the ACC pressure

The pressure data is shown as a function of time, and the polynomial equation is made by the least square method.

(c) Data of the Flow Damper outlet pressure

4) Test Conditions

Visualization Test Conditions

Visualization test conditions are shown in Table 4.2.3-1.

Low Pressure Injection Test Conditions

Low pressure test conditions are shown in Table 4.2.3-2.
The purpose of this test was to confirm the flow characteristics of the flow damper during large flow with wide variations of cavitation factors. The initial pressure conditions for the test tank and the exhaust tank were set at values that facilitated the testing.

Table 4.2.3-1 Visualization Test Conditions

Table 4.2.3-2 Low Pressure Injection Test Conditions

5) Parameters and Measuring Equipment

Pressure, water level and temperature were measured to calculate cavitation factors and flow rate coefficients. The differential pressure transducer measuring water level in tank and the attachments of pressure transducer are shown in Fig. 4.2.3-1.

6) Test Results and Consideration

a) The Visualization Test Results

The visualization test results are listed in Table 4.2.3-3 and the flow in the vortex chamber during large, large/small switching and small flow are shown in Photos. 4.2.3-1 to 4.2.3-3. The white lines are added in the photos to show the tracer trajectories clearly.

(1) The characteristic of the large flow is shown in Photo. 4.2.3-1. Since the flow tracer traveled from the point of the flow from the standpipe directly to the flow damper exit following collision with the water from the small flow inlet, it was confirmed that a vortex was not formed in the vortex chamber during large flow injection.

(2) The characteristic of the large/small flow switching is shown in Photo. 4.2.3-2. It shows transient status forming vortex under flow rate switching. It was also confirmed that gas entrainment from the standpipe did not occur and the flow rate switched smoothly in a short time.

(3) The characteristic of small flow is shown in Photo. 4.2.3-3. It was confirmed that the flow tracer swirled to the outlet, and a stable vortex was formed in the vortex chamber.

Table 4.2.3-3 Visualization Test Results

Test Number (T. No.)	Initial pressure [Test Tank]	Large flow	Flow rate switching	Small flow
1/5- 1-1		A vortex was not formed in the vortex chamber during large flow.	The flow rate switched smoothly in a short time.	-
1/5- 1-2		-	-	A stable vortex was formed in the vortex chamber.
1/5-1-3		-	The flow rate switched smoothly in a short time.	-

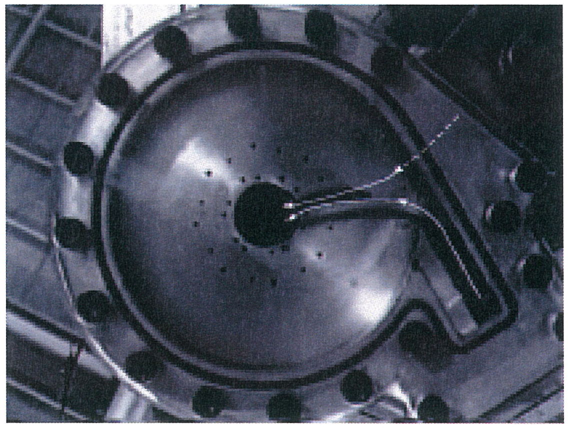

Photo. 4.2.3-1 Large Flow

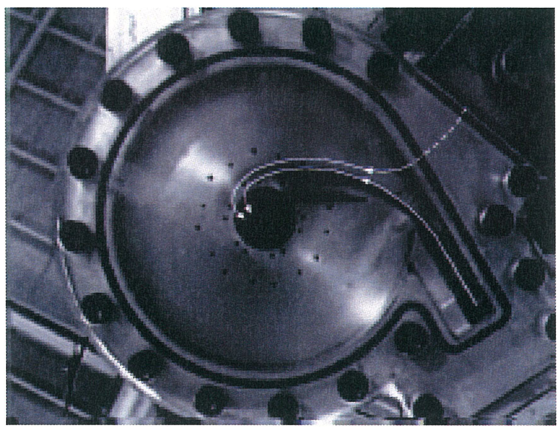

Photo. 4.2.3-2 Switching Flow Rate

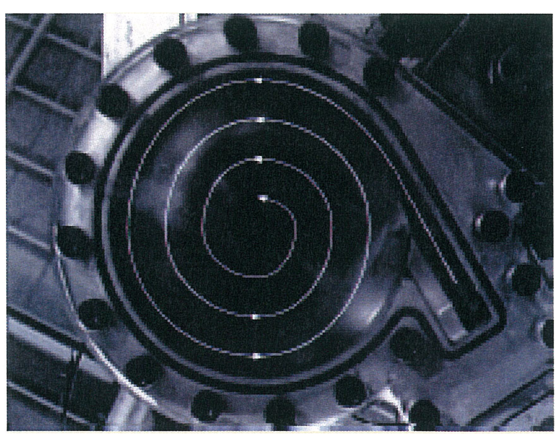

Photo. 4.2.3-3 Small Flow

b) Low Pressure Injection Test Results

This test was conducted at low pressure using a 1/5 scale model and the following results were obtained.

(1) The test tank pressure and water level and the outlet pressure of the flow damper as a function of time are shown in Figs. 4.2.3-2(1/2),(2/2) to 4.2.3-4(1/2),(2/2). It was confirmed that the test tank water level decreased steeply during large flow and decreased gently after the flow rate switching to small flow.

(2) The relation between the flow rate coefficient and cavitation factor in the flow damper is shown in Figs. 4.2.3-2 (2/2) to 4.2.3-4(2/2)[Note]. The behavior of large flow injection shows that the flow rate coefficient increased when the cavitation factor increased and became almost constant when the cavitation factor was greater than[ ].

Note: The data during almost steady condition were plotted.

(3) The relation between the flow rate coefficient and cavitation factor in the flow damper during small flow is also shown. It is shown that the flow rate coefficient during small flow was constant and independent of the cavitation factor.

Fig. 4.2.3-2 (1/2) Low Pressure Injection Test Results (T. No. 1/5-2-1) 1/2

Fig. 4.2.3-2 (2/2) Low Pressure Injection Test Results (T. No. 1/5-2-1) 2/2

Fig. 4.2.3-3(1/2) Low Pressure Injection Test Results (T. No. 1/5-2-2) 1/2

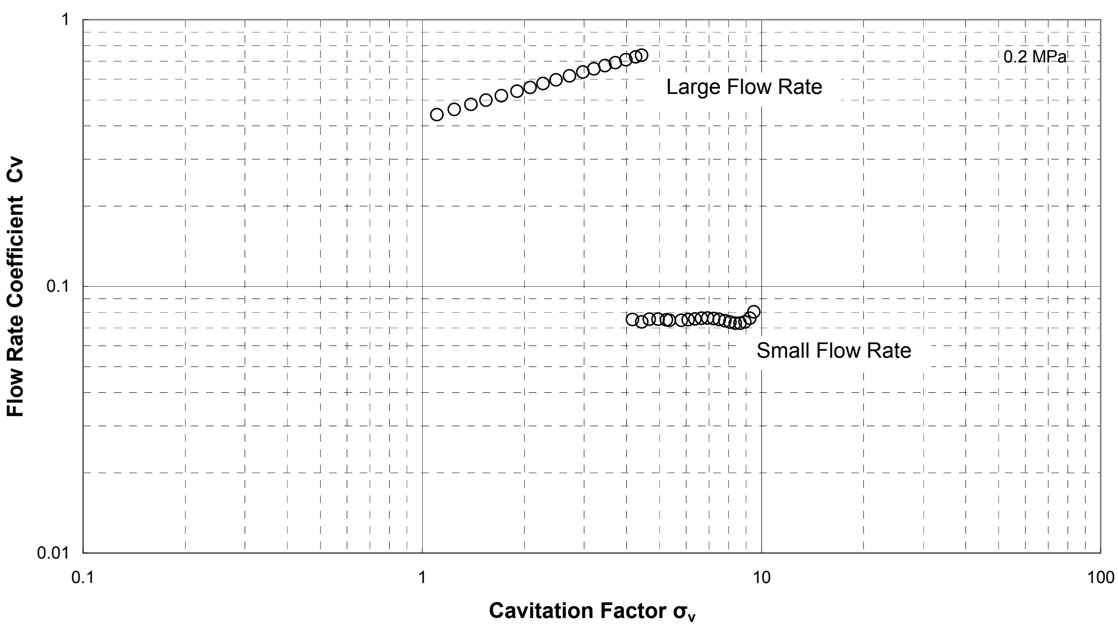

Fig. 4.2.3-3 (2/2) Low Pressure Injection Test Results (T. No. 1/5-2-2) 2/2

Fig. 4.2.3-4 (1/2) Low Pressure Injection Test Results (T. No. 1/5-2-3) 1/2

Fig. 4.2.3-4(2/2) Low Pressure Injection Test Results (T. No. 1/5-2-3) 2/2

4.2.4 Full Height 1/2 Scale Test

1) Objectives

(1) Obtainment of the flow characteristic data and confirmation of no gas entrainment
The test was conducted to obtain the flow characteristic data in the flow damper and to confirm that gas entrainment through the standpipe is prevented during flow switching and small flow injection.

(2) Confirmation that the flow characteristics can be characterized by dimensionless numbers (cavitation factor and flow rate coefficient)
Since a throat was added at the vortex chamber outlet to form strong vortex, it was assumed that cavitation might occur at the throat. The cavitation phenomenon is characterized by the cavitation factor which can be evaluated. It was confirmed by test that the flow rate coefficient is characterized by cavitation factor.

(3) Confirmation of the flow switching water level
The flow rate, as expected, switched from large flow to small flow when the water level decreased to the lower end of the standpipe cap. However, it is assumed that the water switching level may vary in the actual accumulator. Therefore, the actual switching water level was confirmed.

(4) Confirmation of the effect of dissolved nitrogen gas
Since the accumulator tank is pressurized by nitrogen gas, it is assumed that nitrogen gas dissolves into the water. If the water contains dissolved nitrogen gas, the dissolved gas may come out of solution during injection and affect the flow characteristics of the flow damper. Therefore, the test was conducted to evaluate the effect of dissolved gas on the injection flow.

2) Test Facility

The schematic and outline drawing of the test facility and the general flow path are shown in Fig. 4.2.4-1 and Fig. 4.2.4-2. The test facility consists of a test tank, flow damper, injection piping and exhaust tank. The flow damper is installed in the test tank. The height of the test tank and the standpipe is the full scale height and the inner diameter of the test tank is 1/2 scale (Fig. 4.2.4-3 and Fig. 4.2.4-4). Therefore, the water volume is 1/4 scale and the flow rate is also 1/4 scale. The test was conducted simulating the actual time. In addition, the water level transient during flow switching in the standpipe can be observed to represent the level transient in the actual standpipe. A ball valve is provided on the injection line as the isolation valve and a gate valve is provided on the injection line to control flow resistance. A pressure control valve is provided on the upper side of the test tank to control the tank pressure during the test.

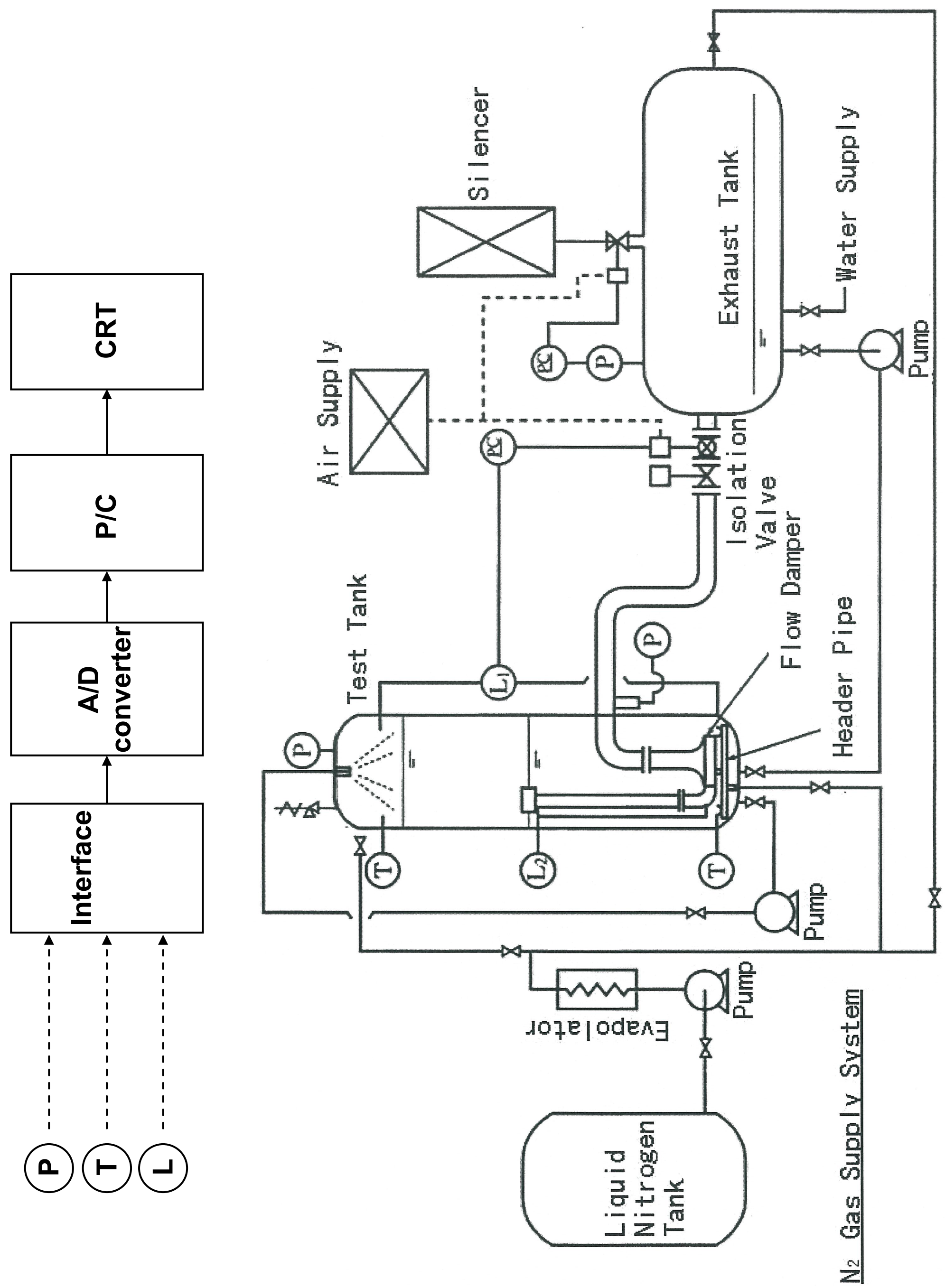

Fig. 4.2.4-1 Schematic Drawing of the Full Height 1/2 Scale Test Facility

Fig. 4.2.4-2 Outline Drawing of the Full Height 1/2 Scale Test Facility

Fig. 4.2.4-3 Schematic Comparison of Actual Tank and Test Tank

Fig. 4.2.4-4 Outline Drawings of the Actual Flow Damper and the Test Flow Damper

3) Test Conditions

Full height 1/2 scale test conditions are shown in Table 4.2.4-1. The following seven cases were tested on initial tank pressure that reflects the ACC operating conditions. And the pressure of the exhaust tank corresponds to RCS pressure.

- Case 1: The initial test tank pressure was 586psig (4.04MPa [gage]) simulating the condition for ECCS performance during a large LOCA.
- Case 2: The initial test tank pressure was 657psig (4.53MPa [gage]) to obtain data for high pressure design.
- Case 3: The initial tank pressure was 758psig (5.23MPa [gage]) to obtain data for high pressure design.
- The pressure in the exhaust tank was 14psig (0.098MPa [gage]) for Case 1, 2, and 3. Since the pressure of the exhaust tank becomes the same as the pressure of the containment vessel (C/V) after the blow down phase during a large LOCA, and ECCS performance analysis uses approximately 14psig(0.098MPa [gage]), the pressure of the backpressure was set at 14psig (0.098MPa [gage]).
- Case 4: The initial tank pressure was the same as Case 1. However, the pressure in the exhaust tank was maintained at 71psig (0.49MPa [gage]) to obtain data for high back pressure.
- Case 5: The test was conducted with water containing dissolved nitrogen to confirm the effect of dissolved nitrogen gas on flow characteristics.
- Case 6: The test was conducted with a small differential pressure between the test tank and the exhaust tank to take into account large cavitation factors.
- Case 7: The injection test was conducted with the initial tank pressure was assuming the pre-operational test condition.
- The valve opening speed was set at seconds which is faster than the depressurization time during a LOCA in order to assure smaller cavitation factors.
- The resistance coefficient of the piping was controlled at the actual design condition in order to confirm the injection time during the large flow injection period.

Table 4.2.4-1 Test Conditions of Full Height 1/2 Scale Test

	Test Tank Pressure	Exhaust Tank Pressure	Initial Gas Volume	Injection Water Volume		Objective
				Large Flow	Small Flow	
	psig [MPa [gage]]	psig [MPa [gage]]	ft^3 [m^3]	ft^3 [m^3]	ft^3 [m^3]	
Case 1	586 (4.04)	14 (0.098)				Obtain flow characteristics for ECCS performance evaluation during a large LOCA
Case 2	657 (4.53)	14 (0.098)				Obtain flow characteristics for high pressure design
Case 3	758 (5.23)	14 (0.098)				Obtain flow characteristics for large differential pressure
Case 4	586 (4.04)	71 (0.49)				Obtain flow characteristics for small differential pressure
Case 5						Obtain flow characteristics to confirm the effect of dissolved nitrogen gas
Case 6						Obtain flow characteristics in large cavitation factors
Case 7						Obtain flow characteristics for the assumed pre-operational test condition

4) Parameters and Measuring Equipment

Pressure, water level, and temperature were measured by the instruments shown in Fig.4.2.4-1 for all test cases and used to calculate the cavitation factor and the flow rate coefficient.

5) Test Results and Conditions

The test results are shown in Figs. 4.2.4-5 to 4.2.4-11. The test results, such as injection flow rate, test tank pressure, test tank water level and the flow rate coefficients [Note] during both large and small flow for each test case, are shown in these figures. The conclusions for each test are shown as follows.

Note: Where possible steady conditions were plotted.

[Case 1]

- It was confirmed that the injection flow rate was switched from large flow to small flow smoothly, and small injection began after large flow injection.[Refer to Fig.4.2.4-5(1/2)]
- It was confirmed that the test tank pressure dropped quickly after initiating the test and dropped gradually, after the flow rate switching at about approximately 114psig (0.8MPa [gage]). [Refer to Fig.4.2.4-5(2/2)]
- It was confirmed that when the test tank water level was reduced to the flow switching level, the standpipe water level temporarily dropped to its low point level in about 1.7 seconds and then recovered and continued to drop gradually during the small flow injection period. [Refer to Fig.4.2.4-5(1/2)]
- It was confirmed that the standpipe water level did not decrease to the top of the flow damper during flow switching. [Refer to Fig.4.2.4-5(1/2)]

[Case 2]

- Although the initial test tank pressure was 71psi (0.49MPa) higher than in Case 1, it was confirmed that the injection flow rate, test tank pressure and water level as a function of time were the same as in Case 1. [Refer to Fig.4.2.4-6(1/2), (2/2)]
- Since the initial test tank pressure was 71psi (0.49MPa) higher than in Case 1, the range of the cavitation factor during large flow shifted slightly to lower side. However, the flow rate coefficient was the same as in Case 1 in the region where the cavitation factor was the same as in Case 1. Therefore, it was confirmed that the characteristics of the flow rate coefficient and the cavitation factor are the same even if the tank pressure was increased 71psi (0.49MPa). [Refer to Fig.4.2.4-6(2/2)]
- It was confirmed that the characteristics of the flow rate coefficient and the cavitation factor during small flow were the same as in Case 1. [Refer to Fig.4.2.4-6 (2/2)]

[Case 3]

- Although the initial test tank pressure was 172psi (1.19MPa) higher than in Case 1, it was confirmed that the injection flow rate, test tank pressure and water level as a function of time were the same as in Case 1. [Refer to Fig.4.2.4-7(1/2), (2/2)]
- The flow rate coefficient was the same as in Case 1 in the performance range where the cavitation factor was the same as in Case 1. Therefore, it was confirmed that the characteristics of the flow rate coefficient and the cavitation factor are the same even if the tank pressure is increased by 172psi (1.19MPa). [Refer to Fig.4.2.4-7(2/2)]

- It was confirmed that the characteristics of the flow rate coefficient and the cavitation factor during small flow were the same as in Case 1. [Refer to Fig.4.2.4-7(2/2)]

[Case 4]

- Although the pressure of the exhaust tank was 71psig (0.49MPa [gage]) as opposed to 14psig (0.098MPa [gage]) in Case 1, it was confirmed that the injection flow rate, test tank pressure, and water level as a function of time were the same as in Case 1. [Refer to Fig.4.2.4-8(1/2), (2/2)]
- The flow characteristics data was obtained over a larger range of cavitation factors than Case 1 because of higher backpressure tank pressure. [Refer to Fig.4.2.4-8(2/2)]

[Case 5]

- For this case, Nitrogen gas was dissolved into the water. It was confirmed that the flow rate coefficient during large flow was smaller than that of the case where nitrogen was not dissolved. [Refer to Fig.4.2.4-9 (2/2)]
- It was confirmed that the flow rate coefficient during small flow was essentially the same as in Case 1 and no change was caused by the dissolved nitrogen gas. [Refer to Fig.4.2.4-9(2/2)]

[Case 6]

- It was confirmed that the injection flow rate was switched from large flow to small flow smoothly, and small injection began after large flow injection. [Refer to Fig.4.2.4-10(1/2)]
- The flow characteristics data was obtained for a larger range of cavitation factors than in Case 1 since the initial test tank pressure was reduced. [Refer to Fig.4.2.4-10(2/2)]

[Case 7]

- Although Case 7 was a low-pressure injection test, it was confirmed that the test tank pressure and water level were reduced rapidly during large flow and that the flow rate switching to small flow reduced gradually, as in Case 1. [Refer to Fig.4.2.4-11(1/2)]
- It was confirmed that the flow characteristics of the flow damper during both large and small flow were consistent with those in other cases. [Refer to Fig.4.2.4-11 (2/2)]

Performance Confirmation during Large Flow

In the case that simulates LOCA conditions, the resistance coefficient during large flow injection is less than[ ]. These results are generally consistent with the performance requirements.

Performance Confirmation during Small Flow

Measurements from the test results of Case 1 show that the flow rate before and after the flow switching was approximately 3170gpm (approximately 720m3/h) and approximately 652gpm (approximately 148m3/h), respectively. Therefore, the flow-switching ratio (3170/652=4.9) was less than[ ]and was consistent with the performance requirements.

Flow Switching Water Level

The measured flow-switching water level in each test case is shown in Table 4.2.4-2. The expected flow-switching water level was set at the lower end of the anti-vortex cap installed at the inlet of the standpipe. The actual flow-switching water levels were within the range from[ ]to[ ]of the expected flow switching water level.

Based on above test results, it was confirmed that the variation of flow-switching water level was limited to a sufficiently small range by the anti-vortex cap at the inlet of the standpipe.

Table 4.2.4-2 Flow Switching Water Level

	Initial tank pressure [psig (MPa [gage])]	Exhaust tank pressure [psig (MPa [gage])]	Flow switching water level [in (mm)][Note]
Case 1	586 (4.04)	14 (0.098)	
Case 2	657 (4.53)	14 (0.098)	
Case 3	758 (5.23)	14 (0.098)	
Case 4	586 (4.04)	71 (0.49)	
Case 5			
Case 6			
Case 7			

Note: Reference point is bottom of anti-vortex cap. The upper is '+', and the lower is '-'.

Water Level Reduction in Switching Flow Rate

It was confirmed that the reduction of the water level in each test during flow switching was smaller than the height of the standpipe and sufficient margin was provided to prevent gas entrainment. [Refer to Fig. 4.2.4-12]

Effect of Dissolved Nitrogen Gas

It was confirmed that, in the test with nitrogen saturated water (Case 5), the duration of large flow injection was slightly longer (approximately [ ]) than in Case 1. Since Case 5 was conducted with nitrogen-saturated water, and this condition was not applicable in the actual accumulator tank, it is assumed that dissolved nitrogen is less effective in the actual tank. [Refer to Fig.4.2.4-9(2/2)]

Result of the Test Assuming Pre-operational Test Condition

The comparison between the characteristics of cavitation factor vs. flow rate coefficient measured in a LOCA simulation test (Case 1) and in this test is shown in Fig. 4.2.4-11. This comparison shows that the cavitation factor over a wide range can be obtained from this test and beyond the results of LOCA simulation test (Case 1). [Refer to Fig.4.2.4-11(2/2)]

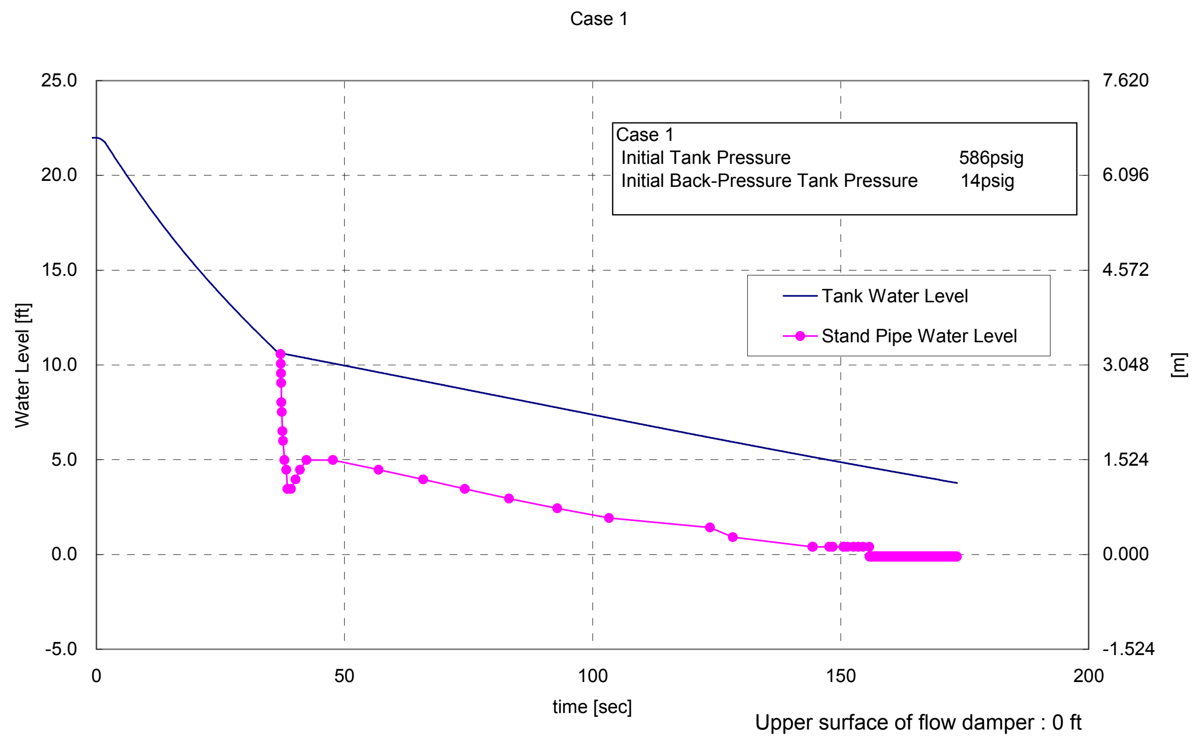

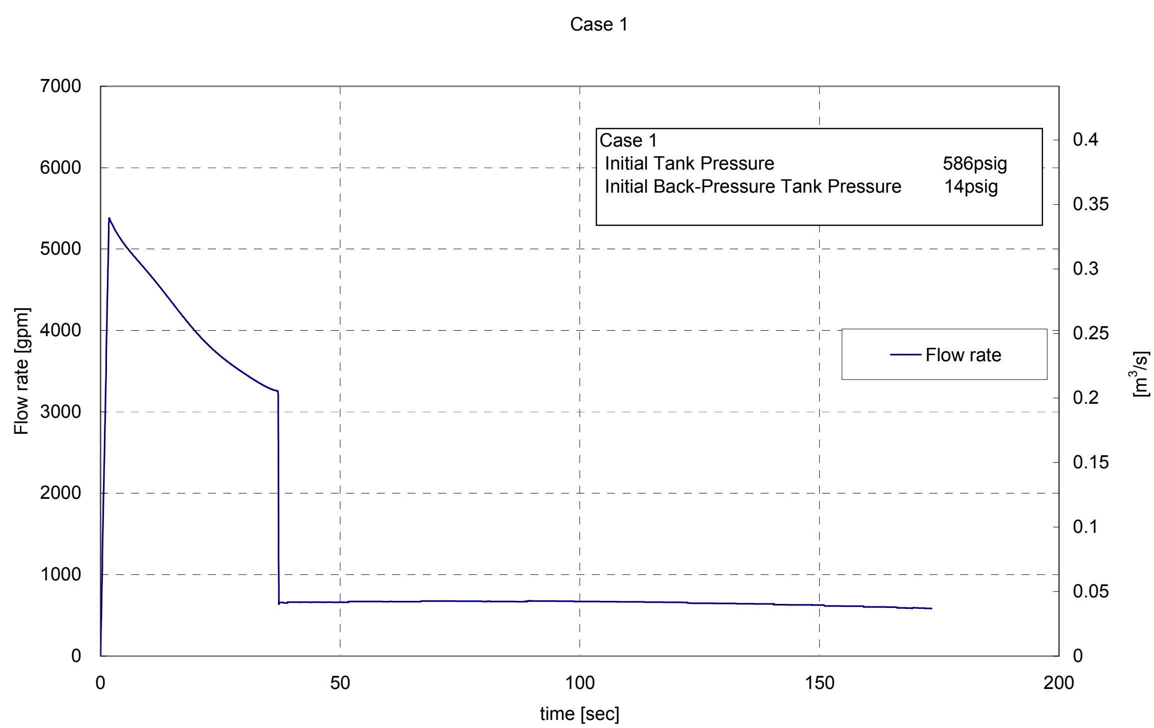

Fig. 4.2.4-5 (1/2) Full Height 1/2 Scale Test Results (Case 1) 1/2

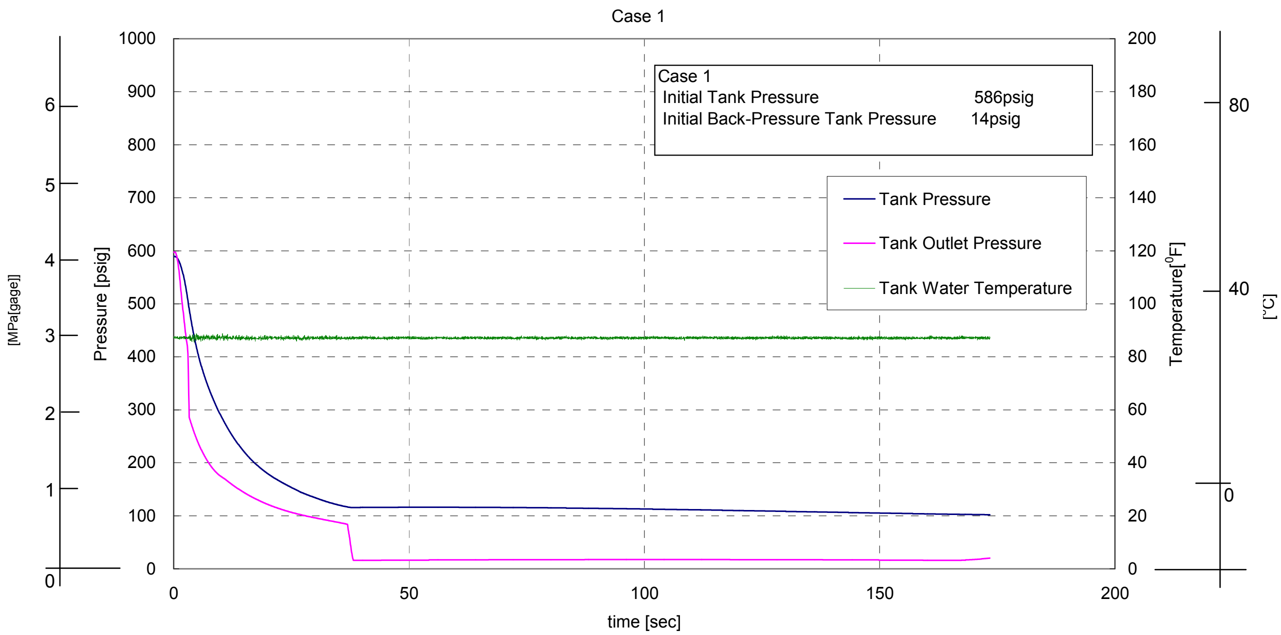

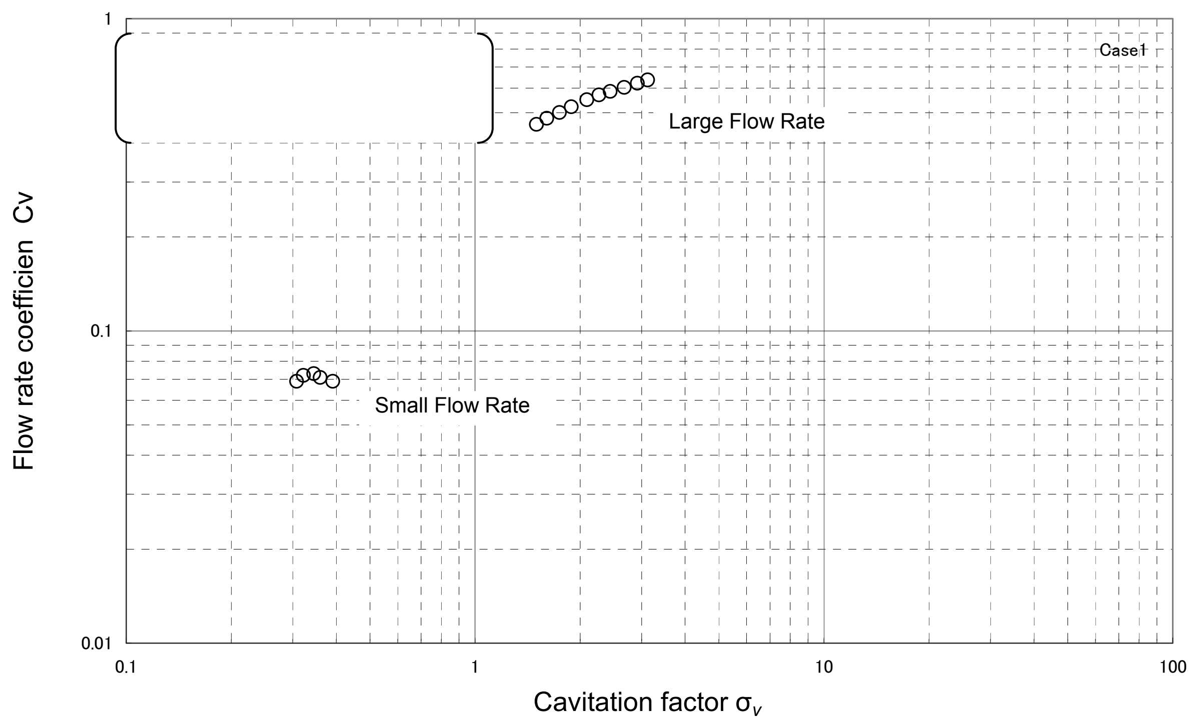

Fig. 4.2.4-5 (2/2) Full Height 1/2 Scale Test Results (Case 1) 2/2

Fig. 4.2.4-6 (1/2) Full Height 1/2 Scale Test Results (Case 2) 1/2

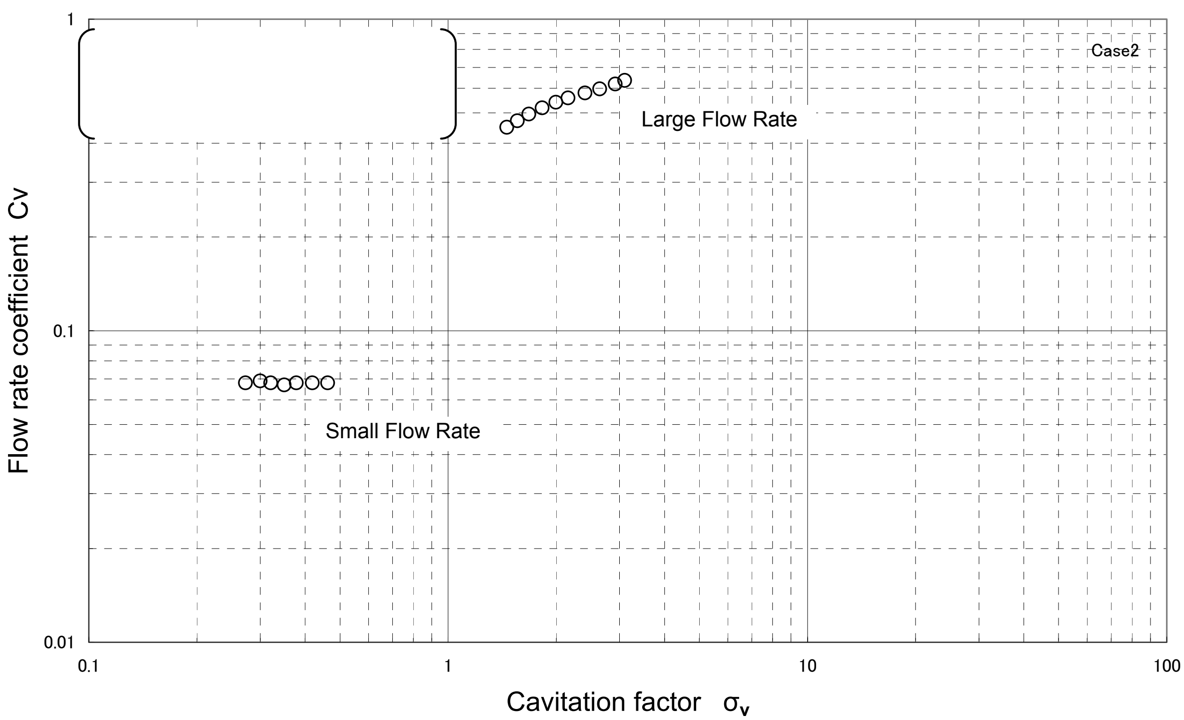

Fig. 4.2.4-6 (2/2) Full Height 1/2 Scale Test Results (Case 2) 2/2

Fig. 4.2.4-7 (1/2) Full Height 1/2 Scale Test Results (Case 3) 1/2

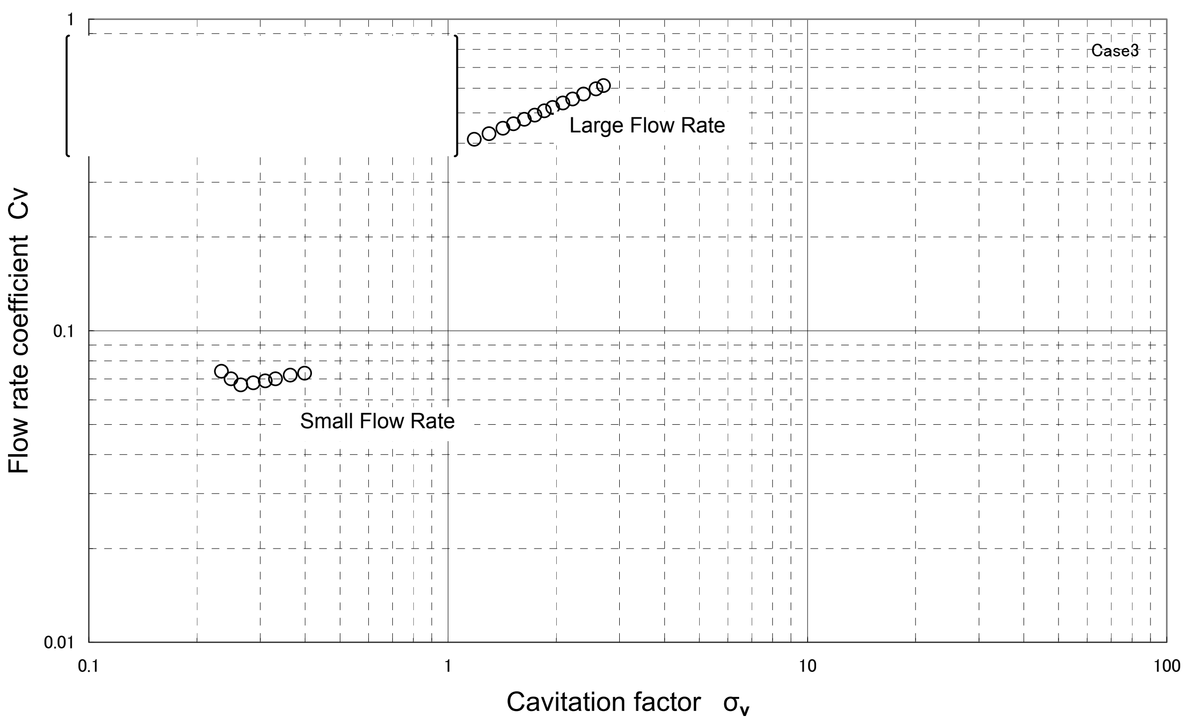

Fig. 4.2.4-7(2/2) Full Height 1/2 Scale Test Results (Case 3) 2/2

Fig. 4.2.4-8 (1/2) Full Height 1/2 Scale Test Results (Case 4) 1/2

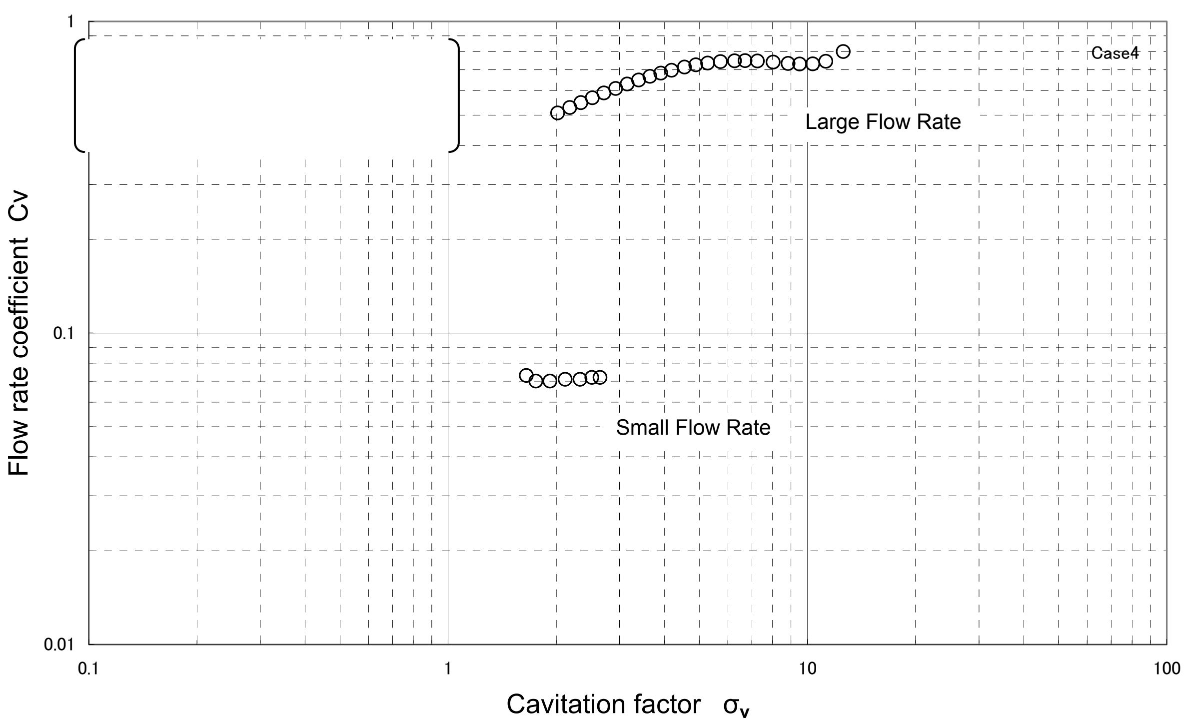

Fig. 4.2.4-8 (2/2) Full Height 1/2 Scale Test Results (Case 4) 2/2

Fig. 4.2.4-9 (1/2) Full Height 1/2 Scale Test Results (Case 5) 1/2

Fig. 4.2.4-9 (2/2) Full Height 1/2 Scale Test Results (Case 5) 2/2

Fig. 4.2.4-10 (1/2) Full Height 1/2 Scale Test Results (Case 6) 1/2

Fig. 4.2.4-10 (2/2) Full Height 1/2 Scale Test Results (Case 6) 2/2

Fig. 4.2.4-11(1/2) Full Height 1/2 Scale Test Results (Case 7) 1/2

Fig. 4.2.4-11(2/2) Full Height 1/2 Scale Test Results (Case 7) 2/2

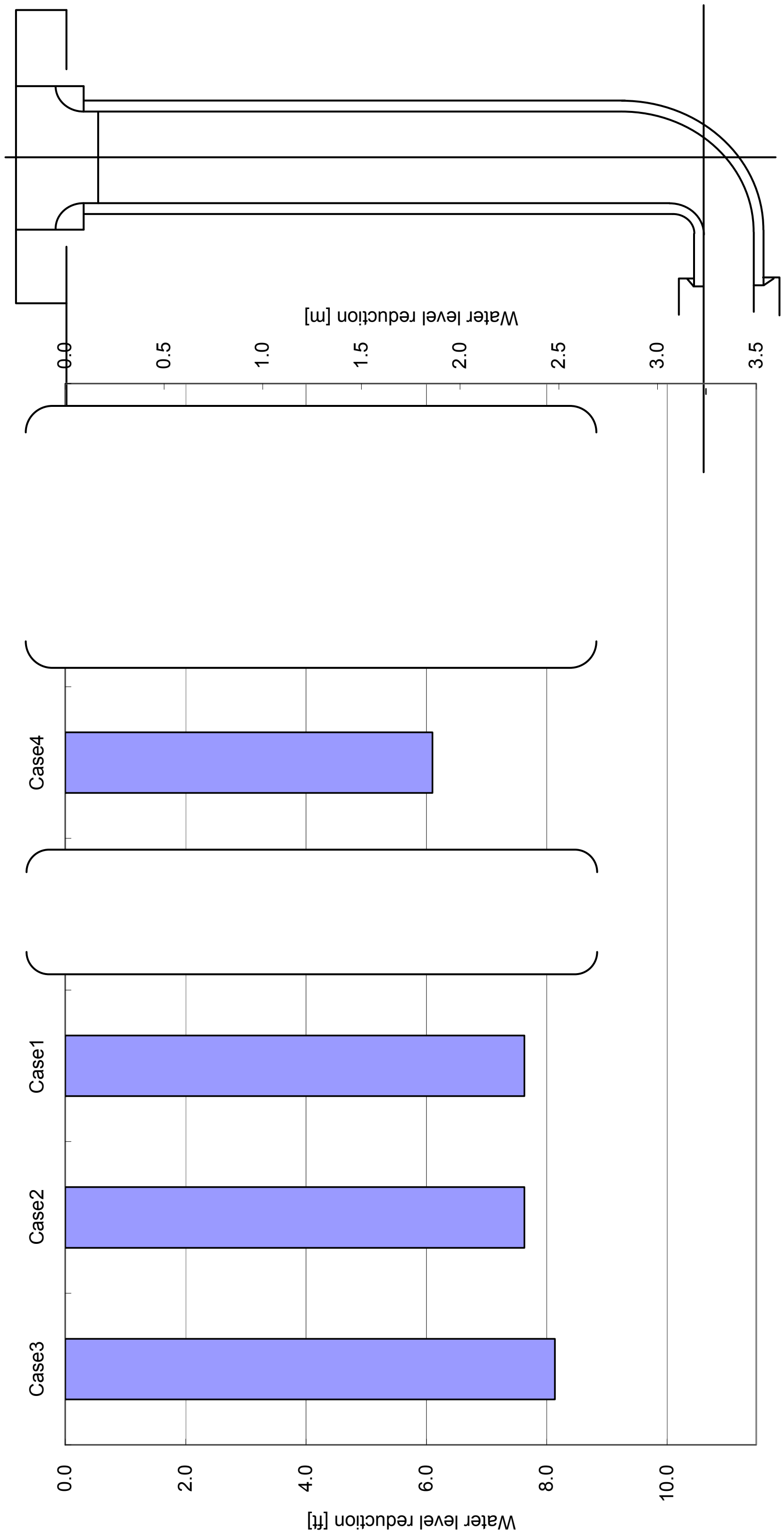

Fig. 4.2.4-12 The Test Results of Water Level Reduction in Switching Flow Rate